



Porous hydroxyapatite scaffold with three-dimensional localized drug delivery system using biodegradable microspheres

Jun Sik Son^a, Mark Appleford^a, Joo L. Ong^a, Joseph C. Wenke^b, Jong Min Kim^c,
Seok Hwa Choi^{c,*}, Daniel S. Oh^{a,**,1}

^a Biomedical Engineering, University of Texas at San Antonio, San Antonio, TX 78249, USA

^b Army Institute of Surgical Research, Fort Sam Houston, TX, USA

^c College of Veterinary Medicine, Chungbuk National University, Republic of Korea

ARTICLE INFO

Article history:

Received 2 July 2010

Accepted 10 March 2011

Available online 21 March 2011

Keywords:

Hydroxyapatite

Poly(lactic-co-glycolic acid)

Drug delivery system

Scaffold

Microsphere

Dexamethasone

ABSTRACT

In this study, ionic immobilization of dexamethasone (DEX)-loaded poly(lactic-co-glycolic acid) (PLGA) microspheres was performed on the hydroxyapatite (HAp) scaffold surfaces. It was hypothesized that *in vivo* bone regeneration could be enhanced with HAp scaffolds containing DEX-loaded PLGA microspheres compared to the use of HAp scaffolds alone. *In vitro* drug release from the encapsulated microspheres was measured prior to the implantation in the femur defects of beagle dogs. It was observed that porous, interconnected HAp scaffolds as well as DEX-loaded PLGA microspheres were successfully fabricated in this study. Additionally, PEI was successfully coated on PLGA microsphere surfaces, resulting in a net positive-charged surface. With such modification of the PLGA microsphere surfaces, DEX-loaded PLGA microspheres were immobilized on the negatively charged HAp scaffold surfaces. Release profile of DEX over a 4 week immersion study indicated an initial burst release followed by a sustained release. *In vivo* evaluation of the defects filled with DEX-loaded HAp scaffolds indicated enhanced volume and quality of new bone formation when compared to defects that were either unfilled or filled with HAp scaffolds alone. This innovative platform for bioactive molecule delivery more potently induced osteogenesis *in vivo*, which may be exploited in implantable bone graft substitutes for stem cell therapy or improved *in vivo* performance. It was thus concluded that various bioactive molecules for bone regeneration might be efficiently incorporated with calcium phosphate-based bioceramics using biodegradable polymeric microspheres.

Published by Elsevier B.V.

1. Introduction

Bone tissue engineering materials has been rapidly developed in recent years as an alternative to autografts and allografts. One of the key components for successful functional tissue-engineered bone regeneration is the presence of scaffolds with optimal architecture for cell migration, differentiation, and interactions. Additionally, the scaffolds have also been used to deliver bioactive factors such as bone morphogenetic proteins and transforming growth factors, thereby enhancing osteoinduction [1]. A functional bone graft substitute in a biocompatible, cell-friendly scaffold mimicking the bone morphology would greatly enhance bone regeneration engineering. Furthermore, use of an innovative bioactive factor loading technique to induce stem cell differentiation would enhance the flexibility of integration into the surrounding tissue.

Since calcium phosphate-based bioceramics such as hydroxyapatite [$Ca_{10}(PO_4)_6(OH)_2$, HAp] is known for its excellent biocompatibility due to its similarity in composition to the apatite found in natural bone [2]. HAp was popularly used for the fabrication of highly porous, interconnected scaffolds and isotropicized pore structure in the last decade [3–5]. Research has also addressed using HAp to specifically deliver stem cell-containing biomaterials to the sites of disease or injury to permit bone regeneration. Although pure HAp is bioactive, it is very difficult to incorporate therapeutic agents within HAp without destroying the biofunctionality of its surface. To overcome this limitation, several composites of HAp and polymers have been developed, such as HAp/chitosan, HAp/polyurethane, HAp/poly(lactic acid), and HAp/poly(lactic-co-glycolic acid) (PLGA). The goal has been to increase mechanical stability and improve tissue interactions by utilizing the excellent bioactive properties of HAp and the biodegradable, easy-processing characteristics of polymers [6–9]. However, these composites have some disadvantages for bone tissue engineering. In particular, polymers used as the main matrix of a composite lack the surface and bulk integration properties to guide cell and tissue growth. Several techniques have been suggested to incorporate therapeutic agents onto porous HAp scaffolds, including

* Corresponding author. Tel.: +82 43 261 3144; fax: +82 43 261 3224.

** Corresponding author. Tel.: +1 210 458 4942; fax: +1 210 458 7007.

E-mail addresses: shchoi@cbu.ac.kr (S.H. Choi), Daniel.oh@utsa.edu (D.S. Oh).

¹ These two authors contributed equally to this work.

Report Documentation Page

*Form Approved
OMB No. 0704-0188*

Public reporting burden for the collection of information is estimated to average 1 hour per response, including the time for reviewing instructions, searching existing data sources, gathering and maintaining the data needed, and completing and reviewing the collection of information. Send comments regarding this burden estimate or any other aspect of this collection of information, including suggestions for reducing this burden, to Washington Headquarters Services, Directorate for Information Operations and Reports, 1215 Jefferson Davis Highway, Suite 1204, Arlington VA 22202-4302. Respondents should be aware that notwithstanding any other provision of law, no person shall be subject to a penalty for failing to comply with a collection of information if it does not display a currently valid OMB control number.

1. REPORT DATE 01 JUL 2011	2. REPORT TYPE N/A	3. DATES COVERED -	
4. TITLE AND SUBTITLE Porous hydroxyapatite scaffold with three-dimensional localized drug delivery system using biodegradable microspheres		5a. CONTRACT NUMBER	
		5b. GRANT NUMBER	
		5c. PROGRAM ELEMENT NUMBER	
6. AUTHOR(S) Son J. S., Appleford M., Ong J. L., Wenke J. C., Kim J. M., Choi S. H., Oh D. S.,		5d. PROJECT NUMBER	
		5e. TASK NUMBER	
		5f. WORK UNIT NUMBER	
7. PERFORMING ORGANIZATION NAME(S) AND ADDRESS(ES) United States Army Institute of Surgical Research, JBSA Fort Sam Houston, TX		8. PERFORMING ORGANIZATION REPORT NUMBER	
		10. SPONSOR/MONITOR'S ACRONYM(S)	
9. SPONSORING/MONITORING AGENCY NAME(S) AND ADDRESS(ES)		11. SPONSOR/MONITOR'S REPORT NUMBER(S)	
		12. DISTRIBUTION/AVAILABILITY STATEMENT Approved for public release, distribution unlimited	
13. SUPPLEMENTARY NOTES			
14. ABSTRACT			
15. SUBJECT TERMS			
16. SECURITY CLASSIFICATION OF:			17. LIMITATION OF ABSTRACT
a. REPORT unclassified	b. ABSTRACT unclassified	c. THIS PAGE unclassified	UU
			18. NUMBER OF PAGES 8
			19a. NAME OF RESPONSIBLE PERSON

dipping the porous HAp scaffold into a solution of the therapeutic agent or coating it with a polymer solution containing therapeutic molecules [10,11]. However, such techniques are inadequate in their control of the long-term drug-release kinetics and can affect the functionality of the HAp surface.

If controlled release from HAp bioceramics is to be achieved, it will require the development of a proper delivery system with respect to the drug-loading efficiency and treatment effectiveness at the target site. Carriers can deliver bioactive growth factors that are essential for the induction of cell differentiation (especially stem cell differentiation) into a specific lineage. Among the various candidates, polymeric microspheres are biodegradable in the human body, display plasticity in fabrication, and have been widely utilized to deliver cytokines and proteins [12,13]. Microspheres enable controlled drug-release kinetics, since their degradation rate can be regulated through the composition of the monomer units and by the microsphere size and morphology [14–16]. Additionally, Dexamethasone (DEX) has been reported to induce the initiation of bone marrow cell differentiation as well as to direct cells toward terminal maturation at the late stages of differentiation [17,18] and thus was used as a model bioactive molecule in this study.

We hypothesized that a novel functional HAp scaffold containing PLGA microspheres loaded with a DEX could serve as an excellent bone substitute material to induce new bone formation *in vivo*. To our knowledge, no one has previously developed bone graft substitutes of inorganic calcium phosphate constructed from organic polymeric microspheres. A simple and highly efficient method is presented for the complete stabilization of the microsphere-based drug delivery structure to the porous HAp scaffold via ionic immobilization. The characteristics and performance of this system were investigated in a pilot preclinical study in beagles.

2. Materials and methods

2.1. Preparation of porous HAp scaffold

Porous HAp scaffold was fabricated using a polymeric template-coating technique as previously described [19]. A polyurethane sponge (60 pores per inch), obtained from E.N. Murray Co. (Denver, CO) was coated with nanoHAp powders (OssGen Co., Daegu, Korea) in distilled water-based slurry. Binders (3% high molecular weight polyvinyl alcohol, 3% carboxymethylcellulose, 5% ammonium polyacrylate dispersant, and 7% *N,N*-dimethylformamide drying agent) were added to the slurry mixture to improve sintering and stabilize the scaffold structure. Coated sponges were dried overnight at room temperature before sintering at 1230 °C for 3 h in a high-temperature furnace. The HAp scaffolds were coated twice with HAp slurry and resintered. Final HAp scaffold dimensions were 5 mm in diameter and 5 mm in length. The morphologies of HAp scaffold produced were observed using a stereoscope (Fisher Micromaster, Fisher Scientific, USA) and scanning electron microscope (SEM; EVO 40, ZEISS, USA). The zeta potential of the HAp scaffold produced was also measured using a particle analyzer (Delsa Nano C, Beckman coulter, USA) at 25 ± 0.5 °C. In preparation for the zeta potential measurement, HAp scaffolds were powdered and suspended in deionized water (1 mg/mL). Particle size of the powdered scaffolds was below 10 µm, with 65% of particles below 1 µm. The zeta potential was then calculated from electrophoretic mobility using Smoluchowski's equation [20].

2.2. Fabrication of DEX-loaded PLGA microspheres

DEX-loaded PLGA microspheres were prepared as previously described [21]. Briefly, PLGA polymer with a lactide/glycolide molar ratio of 75:25 (IV:0.55–0.75 dL/g) was purchased from Boehringer Ingelheim (Ingelheim, Germany), whereas DEX was obtained from Sigma-Aldrich (St. Louis, MO). One milligram of PLGA and 50 mg of DEX, dissolved in 10 mL of a co-solvent of dichloromethane:ethanol (9:1 v/v),

were added to 100 mL aqueous solution of poly(vinyl alcohol) (PVA, 0.2%), followed by emulsification using a homogenizer (powergen 500, Fisher, USA) at 20,000 rpm for 3 min. The emulsified solution was immediately poured into a beaker containing 300 mL of 0.5% PVA solution and stirred with a magnetic stirrer for 4 h in the hood so as to allow the solvent to evaporate. The hardened microspheres were then collected by centrifugation at 3000 rpm for 3 min, washed three times with distilled water, and lyophilized using a freeze dryer. The average size of the fabricated microspheres was determined as estimated from SEM images in three different fields [15].

Similar to the encapsulation of DEX, fabrication of PLGA microspheres to encapsulate Fluorescein isothiocyanate (FITC, Sigma, St. Louis, MO) were performed using the same protocol as described above, except with the addition of 1 mL of FITC (2 mg/mL ethanol) to the PLGA (1 g) solution. The sizes of the FITC-loaded microspheres were observed to be the same as that of the DEX-loaded PLGA microspheres. The samples produced were stored in a desiccator under vacuum at -20 °C for further use.

The polyethyleneimine (PEI, Mw 750,000, Sigma, St. Louis, MO)-coated PLGA microspheres produced were also labeled with FITC using a modification of a previously described technique [22]. PEI-coated microsphere (30 mg/mL) were mixed with FITC (2 mg/mL) in borate buffer (0.1 M, pH 8.5) and incubated at room temperature on a shaker for 2 h. The unbound FITC was removed by centrifugation. The fabrication of FITC-loaded PLGA microspheres and PEI-coated PLGA microspheres labeled with FITC were processed under dark condition. Additionally, the PEI-coated PLGA microspheres labeled with FITC were imaged on a Leica 6000 inverted fluorescence microscope (Leica microsystems, Bannockburn, IL) using ex/em filters of 360/470 nm.

2.3. Immobilization of DEX-loaded PLGA microspheres on the surface of porous HAp scaffold

Immobilization of DEX-loaded and FITC-loaded PLGA microspheres on HAp scaffold surfaces were performed in a three-step process. In the first-step, PLGA microsphere surfaces were radio-frequency (RF) plasma glow-discharged (PDC-32 G, Harrick Plasma, USA) in oxygen-filled chamber at a pressure of 200 mTorr Pa and at 40 mA. The plasma power density and the treatment time were fixed at 30 W and 30 s, respectively. The second step involved dispersing the oxygen plasma-treated PLGA microspheres in the positively-charged linear form of PEI solution (5 mL, 0.05 wt.%) for 12 h at physiological pH. The PEI-coated microspheres were then rinsed three times with distilled water to remove the excess PEI molecules, followed by lyophilizing in a freeze dryer. The final step involved the adding of HAp porous scaffolds to distilled water containing 30 mg of dispersed PEI-coated microspheres, followed by gentle shaking for 4 h. The DEX-loaded PLGA microspheres-immobilized HAp porous scaffold were then washed three times with distilled water to remove the unimmobilized microspheres and dried overnight at room temperature. This method is illustrated in Fig. 1. Using a Leica 6000 inverted fluorescence microscope, HAp scaffold images were generated using an automated z-stack of between 50 and 150 images and color-channel merged for imaging. For amount of microspheres on the surface of HAp, samples were analyzed using thermogravimetry analyzer (TGA; pyris 1, Perkinelmer, USA). Measurements were carried out under a N_2 atmosphere in the temperature range from 30 °C to 600 °C, with a heating rate of 10 °C/min. Analysis of TGA results was performed using pyris software.

2.4. *In vitro* release profile of DEX

Initial concentration of the encapsulated DEX was quantified using a UV spectrophotometer (Synergy2, Biotek, USA) at 235 nm. The loading efficiency (%) was determined based on the ratio of the encapsulated amount of DEX to the initial amount. *In vitro* release

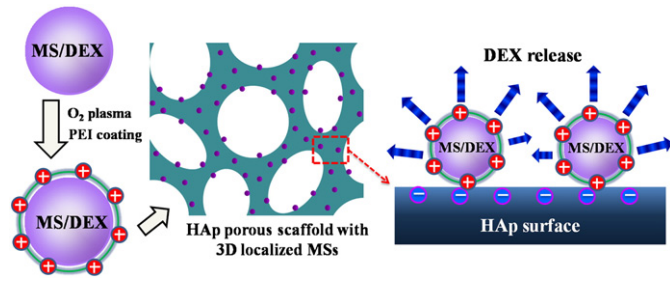


Fig. 1. Schematic diagram of the porous HAp scaffold containing Dex-loaded PLGA microspheres. PLGA microspheres were pre-coated with PEI molecules. The counter-charge of the microsphere and HAp surfaces permitted fabrication of the system via electrostatic interactions.

profile of DEX from the PLGA microspheres immobilized on the HAp scaffold surfaces was also measured by placing the samples in a 3 mL vial and immersing them in 2 mL of phosphate-buffered saline (PBS, pH 7.4) at 37 °C for up to 28 days under static condition. The PBS solution was collected and replaced with fresh PBS at predetermined time interval. The amount of the released DEX was determined by UV spectrophotometer at 242 nm [14].

2.5. *In vivo* study

Three, 2-year-old adult male beagle dogs, weighing 6–9 kg were used to evaluate the *in vivo* performance of DEX-loaded PLGA microspheres immobilized on HA porous scaffold surfaces. Animal selection and management, surgical protocol, and preparation followed routines approved by the Ethical Committee of Animal Experiment, Chungbuk National University Laboratory Animal Research Center (CBNUA-138-1001-01), Chungbuk, Korea. Two 5-mm defects were created in both the left and right femur by retracting the periosteum to expose the surgical sites. Using a trephine drill bit, 5-mm diameter defects were created. The created defects were either filled with control HAp scaffolds, HAp scaffolds immobilized with DEX-loaded PLGA microspheres or left unfilled (controls). Isotropization in the order of implant placement was performed in each beagle. Beagles were then sacrificed at 10 weeks post-surgery and the femurs were collected and placed into 10% neutral buffered formalin.

After sacrifice, the harvested femur was scanned using a computed topography (CT; Hi speed CT/e, GE Medical Co., USA) at 120 kVp and 130 mA, with scan parameter of 1 mm thickness and 512×512 voxel matrix. Hounsfield unit (HU) was measured from the CT scans. Samples were also scanned using micro-computed tomography (micro-CT) SkyScan 1076 (Skyscan, Aartselaar, Belgium) at 100 kV source voltage, 100 μ A source current, and at a spatial resolution of 8.77 μ m. Reconstructions were performed using NRecon software (Skyscan, Aartselaar, Belgium), resulting in grayscale images with a density range from 0.8 to 3.20 gm/cm³ that corresponded to gray scale values of 0 to 255. DataViewer (Skyscan, Aartselaar, Belgium) was used to reslice the CT images along coronal sections which were used to reorient the CT slices to be perpendicular to the axis of the femurs. A region of interest was then generated to only include the cylinder circumscribing the defect plug. The final images were axial slices of the region of interest, which was essentially a 5 mm diameter cylinder from the outer cortical surface to the inner marrow. The total volume of bone ingrowth was computed using CTAn software (Skyscan, Aartselaar, Belgium), whereas the average bone density of the regenerated bone was determined from the mean grayscale value of the pixels included in the binarized selection. Additionally, a slice by slice computation of % bone area per cross sectional area of the region of interest was performed to evaluate the trend of bone regeneration from cortical surface to marrow space within the plug.

2.6. Statistical analysis

All data were expressed as means \pm standard deviation (SD). Statistical difference was analyzed using Student *t* test, and difference was considered significant when *p* value was lower than 0.05.

3. Results

3.1. Materials characterization

As shown in Fig. 2A and B, SEM indicated scaffold architecture with open pores and interconnected rod-like struts. Open channels were observed to be arranged with isotropic geometry and rounded-edge triangular strut morphology. Fig. 2C and D shows the micro-CT images of the scaffold, with complete interconnectivity and having pore size ranging from 230 to 470 μ m and porosity of $88.61 \pm 1.28\%$.

The encapsulation efficiency of DEX to the microspheres was observed to be $10.4 \pm 0.4\%$, with encapsulation efficiency reduced to $7.8 \pm 0.6\%$ after PEI coating. As observed from SEM (Fig. 3A), diameter of the fabricated microspheres ranged from 0.6 to 9 μ m, with the average microsphere diameter being $4 \pm 2.5 \mu$ m. In addition, Fig. 3B shows a representative fluorescence microscopy image of green fluorescing microspheres indicating the positively-charged PEI coating to the negatively charged PLGA microspheres.

3.2. Immobilization of DEX-loaded PLGA microspheres onto HAp scaffold surface

Fig. 4A shows the zeta potential of sintered HAp, DEX-loaded PLGA microspheres, plasma-treated microspheres, and PEI-coated microspheres (parts a–d, respectively), indicating PEI-coated microspheres to be positively-charged and sintered HAp, DEX-loaded PLGA microspheres and plasma-treated microspheres to be negatively charged. Additionally, the zeta potential of O₂ plasma-treated microspheres was observed to be higher than the control microspheres. After suspensions of HAp scaffolds were shaken for 4 h with control or PEI-coated PLGA microspheres, the suspension containing PEI-coated microspheres was clearer than that containing control microspheres (Fig. 4B and C). This result indicated that the PEI-coated microspheres adhered to the HAp scaffold via charge interactions. Fig. 4D shows the immobilization of FITC-loaded microspheres on HAp scaffold surfaces

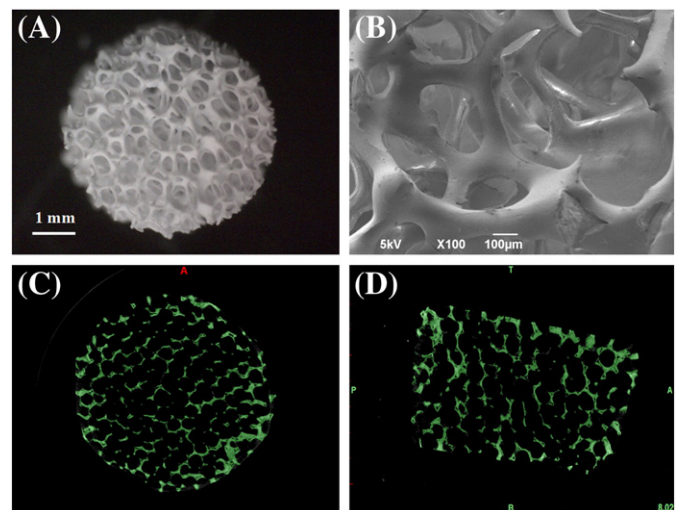


Fig. 2. Various images of HAp porous scaffold. (A) Stereoscope image, (B) SEM image, (C) top and (D) cross-sectional images of HAp architecture from micro-CT.

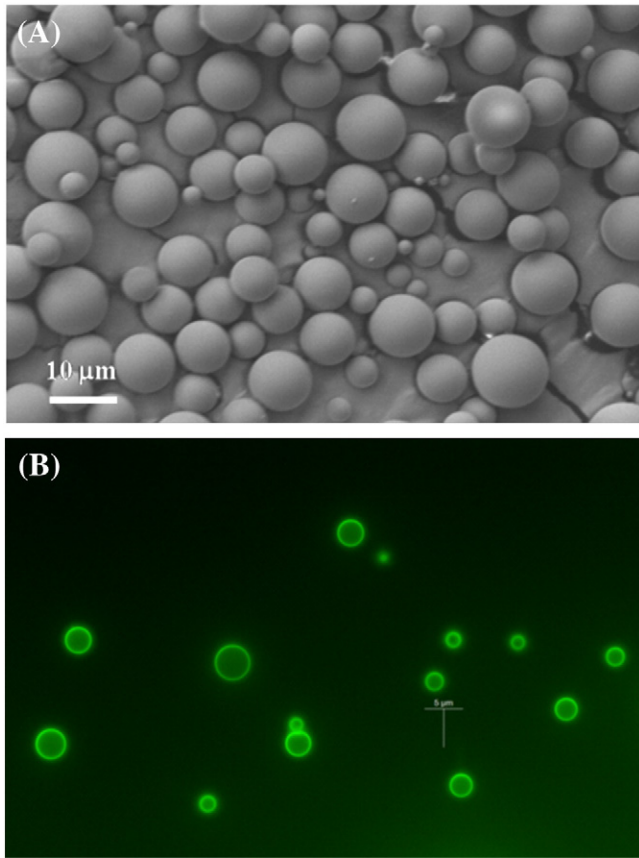


Fig. 3. Morphology and fluorescent images of PLGA microspheres loaded with DEX. (A) SEM image of DEX-loaded PLGA microspheres. (B) Fluorescence microscope image of PEI-coated PLGA microspheres.

in the same manner, and was clearly observed on the scaffold architecture by fluorescence microscopy.

Fig. 5 shows representative SEM images of HAp scaffold surfaces as well as microspheres immobilized on HAp scaffold surfaces. No control microspheres were found on the HAp scaffold surface after 4 h

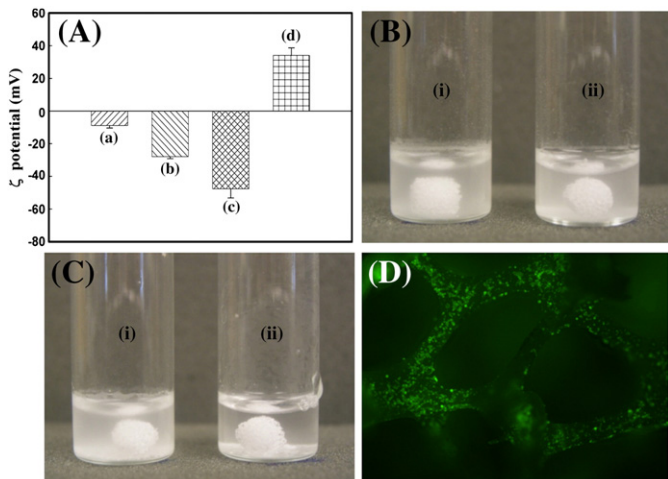


Fig. 4. (A) Zeta potential profile of (a) sintered HAp, (b) control PLGA microspheres, (c) O₂ plasma-treated PLGA microspheres, and (d) PEI-coated PLGA microspheres. (B, C) Digital images of the HAp scaffold in water with dispersed PEI-coated PLGA microspheres before (B) and after (C) shaking for 4 h. (i) Control PLGA microspheres, (ii) PEI-coated PLGA microspheres. (D) Fluorescence microscope image of the HAp scaffold with immobilized PLGA microspheres.

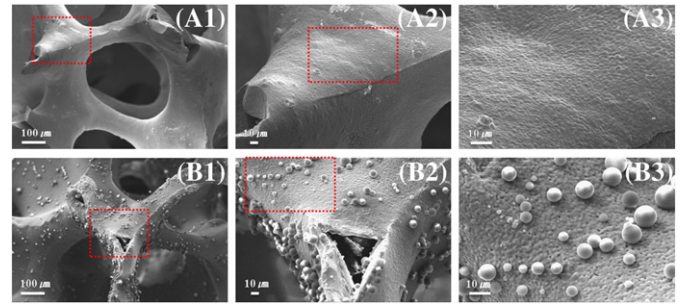


Fig. 5. SEM images of DEX-loaded PLGA microspheres immobilized onto HAp scaffold. (A1–A3) HAp scaffold after shaking for 4 h with water-dispersed control PLGA microspheres. (B1–B3) HAp scaffold after shaking for 4 h with water-dispersed PEI-coated PLGA microspheres.

of mixing (Fig. 5A), while PEI-coated microspheres were well-dispersed and immobilized onto the HAp surface (Fig. 5B).

3.3. Properties of DEX-loaded PLGA microspheres-immobilized porous HAp scaffold

The stability of the microspheres on the surface of HA scaffold in PBS is shown in Fig. 6. SEM revealed the continued presence of microspheres on the surface of HAp throughout the 4 week study, with no appreciable difference in sample appearance at 2 (Fig. 6A) and 4 week (Fig. 6B). However, in comparison to microspheres prior to immersion, changes in the morphology of the PLGA microspheres were observed after immersion in PBS (Fig. 7). The microspheres prior to immersion were observed to be spherical (Fig. 7A), whereas the microspheres were observed to be more flattened over time in solution at the microsphere–HA interface (Fig. 7B and C).

TGA analysis indicated no changes in percent weight residues for HAp alone for temperatures ranging from 30 to 600 °C (a). However, change in percent weight residues was observed for HAp containing microspheres between 200 and 500 °C (b) due to burn-out of the microspheres from the HAp scaffold.

Initial analysis also indicated 0.37 ± 0.16 mg of immobilized microspheres on the HAp scaffold surfaces, with 1.05 ± 0.04 μg DEX. Fig. 8B shows the *in vitro* release profiles of encapsulated DEX from non-immobilized PLGA microspheres and microspheres immobilized on HAp scaffold surfaces. The non-immobilized microspheres showed an early burst of approximately 35% of the total DEX loaded at day 2, followed by a sustained release of the remaining DEX over the next 30 days. In comparison to the non-immobilized microspheres, the release profile from microspheres immobilized on HAp scaffold surfaces showed similar profile but lower amount of DEX released over the study period.

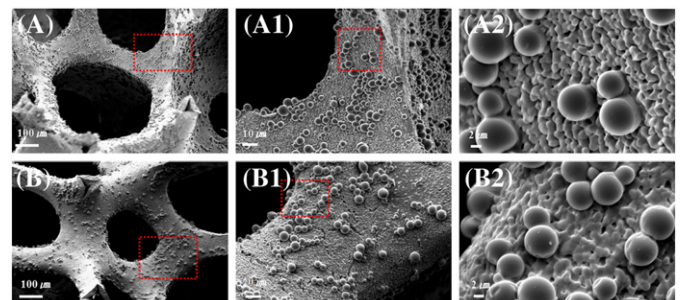


Fig. 6. SEM images of DEX-loaded PLGA microspheres immobilized onto HAp scaffold during incubation in PBS for 2 weeks (A1–A3) or 4 weeks (B1–B3) at 37 °C.

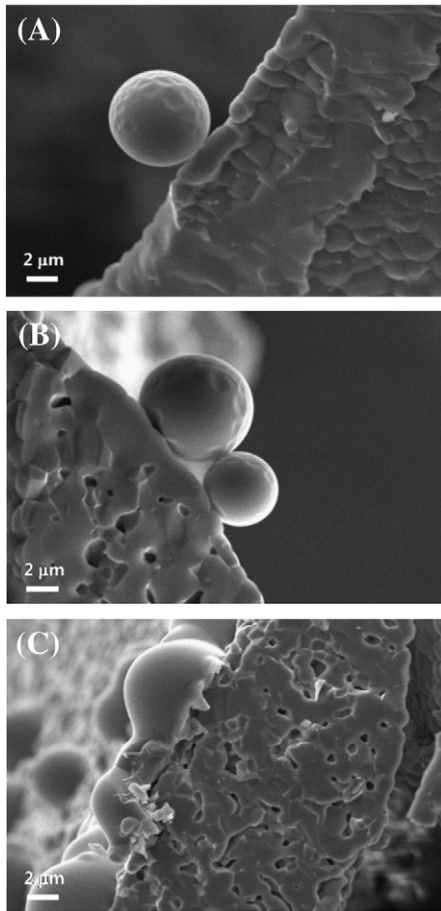


Fig. 7. SEM images of Dex-loaded PLGA microspheres immobilized onto HAp scaffold surface at (A) 0, (B) 2, and (C) 4 weeks in PBS.

3.4. In vivo evaluation of DEX-loaded PLGA microspheres-immobilized HA porous scaffold

At 10 weeks post-implantation, CT analysis revealed the formation of dense cortical bone within both HAp scaffolds and HAp scaffolds with surfaces immobilized with DEX microspheres (Fig. 9A). As shown in Fig. 9A, thin cortical shell bridge was also observed forming across unfilled defects. The HAp scaffold-bone interface became indistinguishable, showing successful engraftment of the scaffolds to bone. The HU value of unfilled defect, defects filled with HAp scaffolds, and defects filled with DEX-loaded HAp scaffolds at 10 weeks post-surgery were measured to be 775 ± 12 , 862 ± 61 , and 1042 ± 28 , respectively (Fig. 9B), indicating significantly higher bone density of defect sites filled with DEX-loaded HAp scaffolds compared to unfilled defects and defects filled with HAp scaffolds.

Fig. 10 showed micro-CT images and 3D volume reconstruction of filled and unfilled defects. In agreement to CT analysis, the unfilled defects revealed the formation of a thin cortical shell bridge across the defect, with incomplete healing (Fig. 10A). For defects filled with HAp scaffold, new bone formation in the open scaffold pores, with incomplete healing was observed (Fig. 10B). Defects filled with DEX-loaded microspheres immobilized on HAp scaffold indicated new bone formation with complete healing after 10 weeks post-implantation (Fig. 10C). According to the 3D volume images (Fig. 10A1–C1), dense bone regenerated into the functional HAp scaffold more than into the control HAp scaffold.

Fig. 11A shows that the bone volume/total volume of unfilled defects, defects filled with HAp scaffolds, and defects filled with DEX-loaded HAp scaffolds were observed to be 40.10 ± 1.88 , 61.62 ± 2.50 , and 63.84 ± 5.46 , respectively. No significant difference in the bone

volume was observed between defects filled with HAp scaffolds and defects filled with DEX-loaded HAp scaffolds. Fig. 11B shows a significantly higher bone mineral density in defects filled with DEX-loaded HAp scaffolds compared to defects that were either unfilled or filled with HAp scaffolds. These results indicate that the volume and quality of new bone formation was significantly improved by the incorporation of DEX-loaded PLGA microspheres into the porous HAp scaffold.

4. Discussion

A novel porous HAp scaffold with incorporated drug-releasing PLGA microspheres was developed as a drug delivery platform for bone regeneration. To develop this combination system, we manipulated the charge interaction between the HAp and PLGA microsphere surface, which resulted in complete localization of the drug delivery structure to the porous HAp scaffold. Both PLGA and HAp are negatively charged at physiologic pH due to the presence of a carboxyl group and phosphate components, respectively [23,24]. In contrast, the PEI polymer has a strong positive charge [25]. Therefore, PEI-coated PLGA microspheres were immobilized on the HAp surfaces via electrostatic interactions. Park et al. successfully designed dual drug-eluting PLGA double-bead microspheres by utilizing the ionic interaction between small, negatively charged PLGA microspheres and large, positively-charged microspheres that were pre-coated with PEI.

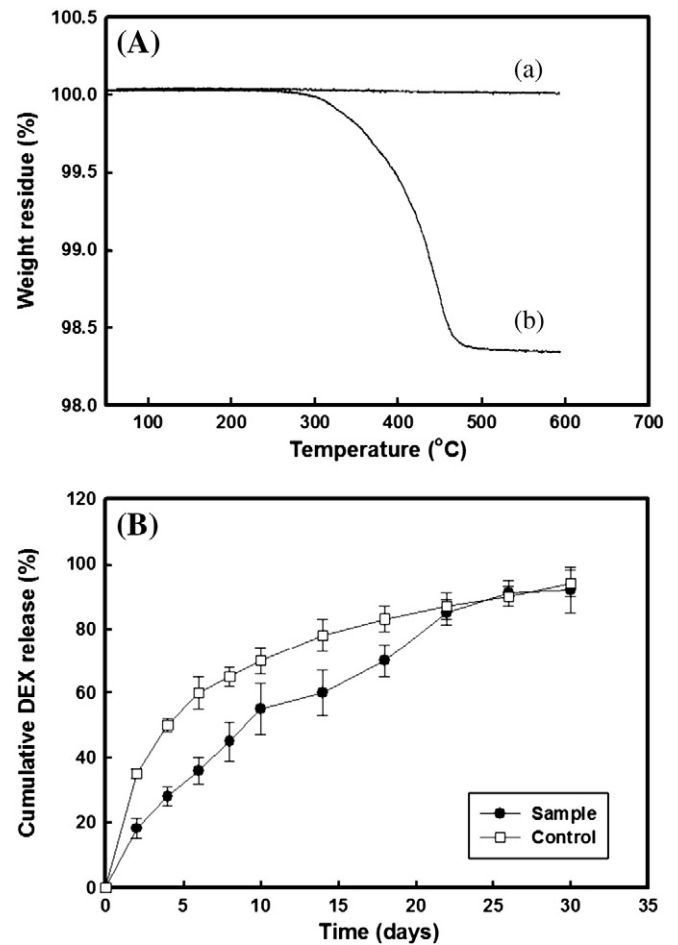


Fig. 8. TGA curve (A) and release profile (B) of DEX from PLGA microspheres immobilized onto HAp scaffold. HAp scaffold without PLGA microspheres (a) and with PLGA microspheres (b). (□) Control PLGA microspheres, (●) PLGA microspheres immobilized to the HAp scaffold.

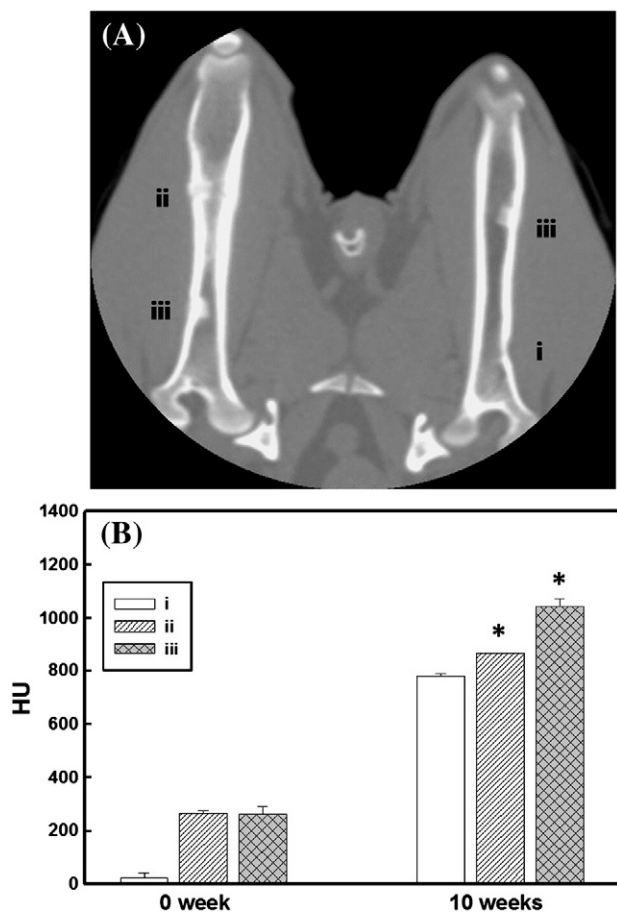


Fig. 9. Computed tomography (A) and HU profile (B) of (i) empty defect (without HAp), (ii) control HAp (without microspheres), and (iii) Dex-loaded PLGA microspheres immobilized onto HAp scaffold at 10 weeks post-implantation in the beagle femur with 5-mm drill hole defects. * $p < 0.05$.

Drug delivery systems using polymeric microspheres are widely utilized to deliver various bioactive molecules for biological application, and offer a broad range of systems with delivery rates that can be modulated over the required time period (from several days to several months) [26,27]. In particular, PLGA is a bioabsorbable polymer with a long history of safe use in medical applications. For clinical use, the PLGA particle can be manufactured in pyrogen-free form under good manufacturing practice guidelines. Recently, PLGA microparticles have been developed that incorporate PEI to enhance pDNA delivery to cells and to help control BMP-2 delivery kinetics by utilizing the counter charges between PEI and negatively charged genes [28–31]. However, such PLGA microspheres have not been truly applied in calcium phosphate-based bioceramics such as HAp or tricalcium phosphate (TCP). Therefore, biodegradable PLGA microspheres may be useful as a drug delivery vehicle by incorporating bioactively loaded microspheres into the porous HAp scaffold architecture.

The functional HAp scaffold system described in this paper offers several advantages. Compared with the coating method, microsphere binding technology can more effectively incorporate drugs or multi-drugs onto the HAp scaffold without destroying the surface biological features. PLGA microspheres retained in the cytoplasm or extracellular spaces release the encapsulated drug slowly in conjunction with the hydrolysis and drug diffusion from the microspheres. This slow intracellular release might result in sustained intracellular drug delivery. These advantages likely contribute to the highly efficient targeted delivery of drugs eluted from the microsphere-incorporated HAp scaffold. Therefore, our combination system of PLGA microspheres and a porous HAp scaffold provides an innovative platform for

delivering bioactive molecules in the future treatment of bone injury or disease.

HAp has good biocompatibility and osteoconductive capacities [32,33]. Compared with other bone substitutes (e.g., collagen scaffolds), HAp is characterized by its precisely defined physical and chemocrystalline properties, high level of purity, and uniformity of chemical composition, so that its biological reactions can be predicted reliably [34]. HAp can be fabricated into high porosity scaffolds with good interconnectivity, which will ensure intercellular communication among osteogenic cells rested in the lacunae [35,36]. We previously fabricated a highly porous HAp scaffold with interconnected pores via the polymer template-coating technique, and demonstrated that this scaffold was successfully mineralized with bone and vascularized in a canine defect model at 12 weeks post-implantation [37]. In the present study, polyurethane template-coating was used to create a HAp scaffold with a controllable pore size and good pore interconnectivity. This scenario creates a friendly structure for cells and tissues that is similar to the natural bone structure.

To functionalize the macromolecules on the highly porous HAp scaffold, Dex-loaded biodegradable PLGA microspheres were fabricated by a standard water/oil emulsion method. The produced microspheres had a nano- to sub-micron diameter that did not significantly affect the porosity or interconnectivity of the functional HAp scaffold. The size of the microsphere immobilized onto the HAp surface is an important factor for maintaining good geometrical and biological properties. In addition, by offering a larger surface area, nano-sized particles are more beneficial for drug delivery than micro-sized particles.

Plasma treatment is widely used to modify the PLGA scaffold surface to improve cell affinity [38,39]. Interestingly, the zeta potential of O_2 plasma-treated microspheres was higher than that of control microspheres. Hydrophilic surface modification of the PLGA microsphere by plasma treatment allows effective PEI coating on the microsphere surface by permitting the PEI molecules to easily approach and interact with the PLGA surface by the enhanced surface charge.

On the other hand, the release kinetics of DEX from immobilized microspheres on the surface of HA scaffold and non-immobilized microspheres (control) followed almost zero-order release. The release profile of both the microspheres exhibited linear release patterns at an early stage and slower release patterns at a later stage. The first order release kinetic rate was due to the diffusion of DEX in the outer surface of microspheres and slower release at the later stage was due to the gradual depletion of DEX in the polymer phase. Since there was no significant change in surface of the microspheres during

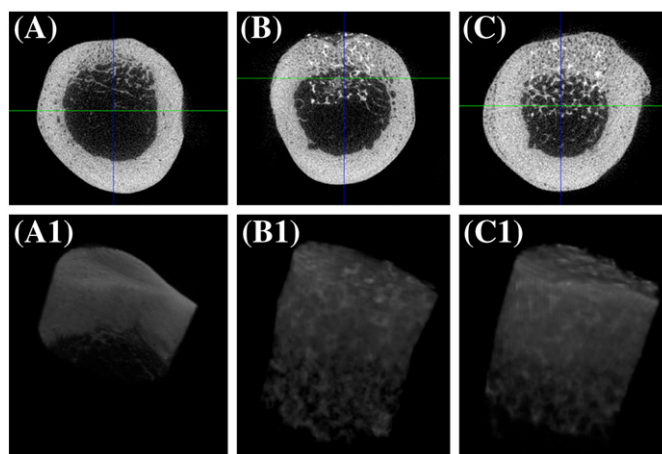


Fig. 10. Axial and 3D images of micro-CT of (A, A1) empty defect (without HAp), (B, B1) control HAp (without microspheres), and (C, C1) DEX-loaded PLGA microspheres immobilized onto HAp scaffold at 10 weeks post-implantation in beagle femurs with 5-mm drill hole defects.

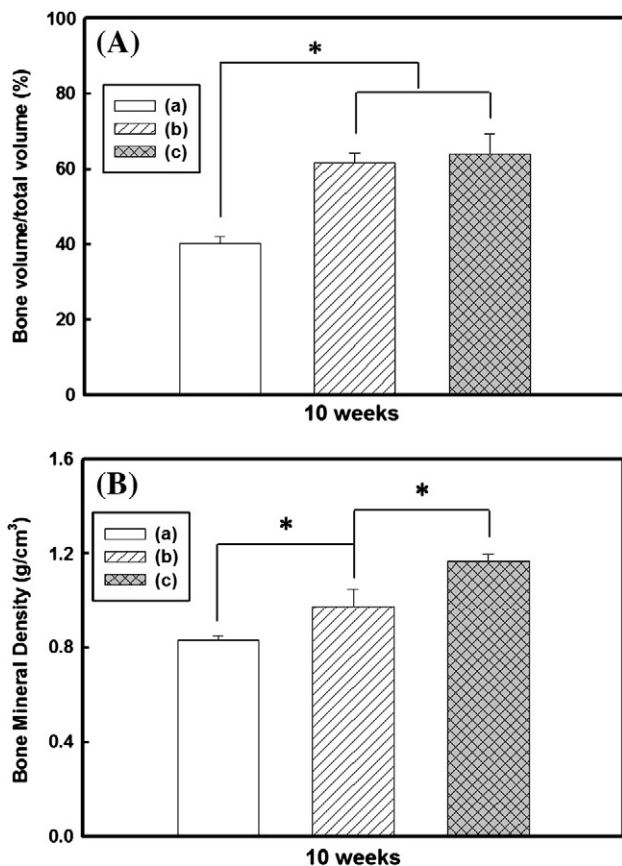


Fig. 11. Bone volume (A) and bone mineral density (B) profiles of (a) empty defect (without HAP), (B) control HAP (without microspheres), and (C) Dex-loaded PLGA microspheres immobilized onto HAP scaffold at 10 weeks post-implantation in beagle femurs with 5-mm drill hole defects. * $p < 0.05$.

the incubation period for 4 weeks (Fig. 7), it is reasonable to say that the sustained release of DEX took place mainly by controlled molecular diffusion of DEX through the PLGA polymer phase, not by either a dissolution controlled or an erosion controlled mechanism [40,41]. Brochhausen et al. reported that the 85:15 type PLGA microspheres are slowly degrading from the inside due to the formation of a superficial diffusion barrier and shows nearly no superficial erosion even after 80 days in culture medium [42].

DEX induces the initiation of osteogenic differentiation of bone marrow stromal cells (MSCs) at an early stage and directs the cells towards terminal maturation at the late stages of differentiation [17]. Thus, the continuous exposure of MSCs to DEX via the sustained release of DEX from PLGA microspheres causes MSCs to differentiate into mature osteoblasts. However, DEX has potentially adverse effects, particularly when administered systemically at high doses for long periods of time [43]. We tried to minimize the adverse effects of DEX by localizing DEX to the tissue-engineered sites.

Some studies suggested that the effective concentration of DEX for the osteogenic differentiation of MSCs was in the range of 10 nM (40 ng/mL) to 100 nM (400 ng/mL) and showed toxic effects at 1000 nM (4000 ng/mL) [44,45]. In our system, the HA scaffold containing microsphere in presented study, was expected release daily dose of approximately under 100 ng of DEX based on the drug-release profile and this was actually within the scope of the *in vivo* study [18].

To determine the DEX content, we successfully used TGA to measure the quantity of microspheres in the HAP scaffold. This result indicated that DEX content could be controlled effectively, which is beneficial to cells infiltrating or migrating into the implanted HAP scaffold in the body. The microsphere stability on the HAP scaffold surface was evaluated over 4 weeks and revealed a similar presence of

the PLGA microspheres at 2 and 4 weeks. DEX was successfully released by the degradation of microspheres on the HAP surface. These results show that various bioactive molecules for bone regeneration can be efficiently incorporated with calcium phosphate-based bioceramics using biodegradable polymeric microspheres. The release kinetics of these molecules can be efficiently tuned through the application of microsphere drug capture technology on the porous HAP scaffold.

To evaluate the *in vivo* performance of our drug delivery system, femur defects in beagles were filled with control HAP without microspheres, functional HAP scaffolds with Dex-loaded microspheres, or left unfilled as an empty defect without HAP. During the 10-week observation period, the functional HAP scaffold more avidly induced osteogenesis than the empty defect or control HAP scaffold. It is presumed that the mechanism for this effect was that DEX was locally released from PLGA microspheres into the open and interconnected architecture space of HAP. This release caused cells to proliferate, differentiate, produce ECM, and form tissues *in vivo* [46]. Previous reports suggested that sustained delivery of low doses of DEX might enhance osteogenesis [47,48]. Therefore, we believe that cells in defect site filled with functional HAP scaffold which have low doses of DEX as mentioned above, would be considered to be exposed to effective DEX concentration, leading to increased osteogenesis *in vivo*. For effective bone tissue engineering, the optimal concentration of DEX in the HA scaffold should be determined by further experimentation because as yet the *in vivo* release behaviors and the *in vivo* clearance rates of DEX are unknown.

The results of the present study indicate that a functional HAP scaffold with a 3D-localized drug delivery system using polymeric microspheres serves as a clinically effective bone graft material to induce osteogenesis *in vivo*. Our combination system could be used to deliver multiple agents with different time courses from the microsphere-containing HAP scaffold. Since the bioabsorption time of PLGA polymer in the living body is controlled by the molecular make-up of PLGA, the time course of intracellular drug delivery can be carefully tuned. Although these results have indicated enhanced bone regeneration *in vivo*, clinical effectiveness of such a system in patients remains to be evaluated.

5. Conclusion

A functional porous HAP scaffold containing 3D-localized drug delivery structures (polymeric microspheres) was successfully developed as an excellent drug delivery platform for bone regeneration. DEX as a model bioactive molecule was efficiently added to the microsphere-containing porous HAP scaffold without biological malfunctions, and the release kinetics of DEX could be efficiently tuned through microsphere capture technology. *In vivo* evaluation of the defects filled with DEX-loaded HAP scaffolds indicated enhanced volume and quality of new bone formation when compared to defects that were either unfilled or filled with HAP scaffolds alone. Consequently, this newly developed drug-loaded PLGA microsphere-immobilized HAP scaffold system might be applicable as a promising scaffold for bone regeneration.

Acknowledgements

This study was supported in part by the Department of Defense funds and the Orthopaedic Extremity Trauma Research Program grants (USAMRMC # W81XWH-08-1-0393 and W81XWH-07-1-0717).

References

- [1] E.H. Groeneveld, J.P. Van den Bergh, P. Holzmann, C.M. Bruggenkate, D.B. Tuinzing, E.H. Burger, Mineralization processes in demineralized bone matrix grafts in human maxillary sinus floor elevations, *J. Biomed. Mater. Res.* 48 (1999) 393–402.

- [2] W. Suchanek, M. Yoshimura, Processing and properties of hydroxyapatite-based biomaterials for use as hard tissue replacement, *J. Mater. Res.* 13 (1998) 94–117.
- [3] K.A. Hing, S.M. Best, K.E. Tanner, W. Bonfield, Quantification of bone ingrowth within bone-derived porous hydroxyapatite implants of varying density, *J. Mater. Sci. Mater. Med.* 10 (1999) 663–670.
- [4] D.M. Liu, Fabrication and characterization of porous hydroxyapatite granules, *Biomaterials* 17 (1996) 1955–1957.
- [5] S.H. Li, J.R. Wijn, P. Layrolle, K. de Groot, Synthesis of macroporous hydroxyapatite scaffolds for bone tissue engineering, *J. Biomed. Mater. Res.* 61 (2002) 109–120.
- [6] I. Kong, Y. Gao, W. Gao, Y. Gong, N. Zhao, X. Zhao, Preparation and characterization of nano-hydroxyapatite/chitosan composite scaffold, *J. Biomed. Mater. Res.* 75 (2005) 275–282.
- [7] L. Wang, Y. Li, Y. Zuo, L. Zhang, Q. Zou, L. Cheng, H. Jiang, Porous bioactive scaffold of aliphatic polyurethane and hydroxyapatite for tissue regeneration, *Biomed. Mater.* 4 (2009) 1–7.
- [8] G. Wei, G.P. Ma, Structure and properties of nano-hydroxyapatite/polymer composite scaffolds for bone tissue engineering, *Biomaterials* 25 (2004) 4749–4757.
- [9] Y.C. Fu, H. Nie, M.L. Ho, C.K. Wang, C.H. Wang, Optimized bone regeneration based on sustained release from three-dimensional fibrous PLGA/Hap composite scaffolds loaded with BMP-2, *Biotechn. Bioeng.* 99 (2008) 996–1006.
- [10] W. Paul, C.P. Sharma, Development of porous spherical hydroxyapatite granules: application towards protein delivery, *J. Mater. Sci. Mater. Med.* 10 (1999) 383–388.
- [11] H.W. Kim, J.C. Knowles, H.E. Kim, Hydroxyapatite/poly(ϵ -caprolactone) composite coatings on hydroxyapatite porous bone scaffold for drug delivery, *Biomaterials* 25 (2004) 1279–1287.
- [12] X.Q. Zhang, J. Intra, A.K. Salem, Comparative study of poly(lactic-co-glycolic acid) poly ethyleneimine-plasmid DNA microparticles prepared using double emulsion methods, *J. Microencaps.* 25 (2008) 1–12.
- [13] T.P. Richardson, M.C. Peters, A.B. Ennett, D.J. Mooney, Polymeric system for dual growth factor delivery, *Nat. Biotechnol.* 19 (2001) 1029–1034.
- [14] S.E. Bae, J.S. Son, K. Park, D.K. Han, Fabrication of covered porous PLGA microspheres using hydrogen peroxide for controlled drug delivery and regenerative medicine, *J. Control. Release* 133 (2009) 37–43.
- [15] S.H. Choi, T.G. Park, G-CSF loaded biodegradable PLGA nanoparticles prepared by a single oil-in-water emulsion method, *Int. J. Pharm.* 311 (2006) 223–228.
- [16] H.K. Kim, H.J. Chung, T.G. Park, Biodegradable polymeric microspheres with “open/closed” pores for sustained release of human growth hormone, *J. Control. Release* 112 (2006) 167–174.
- [17] R.M. Porter, W.R. Huckle, A.S. Coldstein, Effect of dexamethasone withdrawal on osteoblastic differentiation of bone marrow stromal cells, *J. Cell. Biochem.* 90 (2003) 13–22.
- [18] H. Kim, H. Suh, S.A. Jo, H.W. Kim, J.M. Lee, E.H. Kim, Y. Reinwald, S.H. Park, B.H. Min, I. Jo, In vivo bone formation by human marrow stromal cells in biodegradable scaffolds that release dexamethasone and ascorbate-2-phosphate, *Biochem. Biophys. Res. Commun.* 332 (2005) 1053–1060.
- [19] M.R. Appleford, S. Oh, J.A. Cole, J. Protivínský, J.L. Ong, Ultrasound effect on osteoblast precursor cells in trabecular calcium phosphate scaffolds, *Biomaterials* 28 (2007) 4788–4794.
- [20] A. Sze, D. Erickson, L. Ren, D. Li, Zeta-potential measurement using the smoluchowski equation and the slope of the current-time relationship in electroosmotic flow, *J. Colloid Interface Sci.* 261 (2003) 402–410.
- [21] T. Hickey, D. Kreutzer, D.J. Burgess, F. Moussy, In vivo evaluation of a dexamethasone/PLGA microsphere system designed to suppress the inflammatory tissue response to implantable medical devices, *J. Biomed. Mater. Res.* 61 (2002) 180–187.
- [22] M. Feng, D. Lee, P. Li, Intracellular uptake and release of poly(ethyleneimine)-copoly(methylmethacrylate) nanoparticle/pDNA complexes for gene delivery, *Int. J. Pharm.* 311 (2006) 209–214.
- [23] K. Na, S. Kim, K. Park, K. Kim, D.G. Woo, I.C. Kwon, H.M. Chung, K.H. Park, Heparin/poly(L-lysine) nanoparticle-coated polymeric microspheres for stem-cell therapy, *J. Am. Chem. Soc.* 129 (2007) 5788–5789.
- [24] I.O. Smith, M.J. Baumann, L. Obadia, J.M. Boulter, Surface potential and osteoblast attraction to calcium phosphate compounds is affected by selected alkaline hydrolysis processing, *J. Mater. Sci. Mater. Med.* 15 (2004) 841–846.
- [25] G. Wang, K. Siggers, S. Zhang, H. Jiang, Z. Xu, R.F. Zernicke, J. Matyas, H. Uludag, Preparation of BMP-2 containing bovine serum albumin (BSA) nanoparticles stabilized by polymer coating, *Pharm. Res.* 25 (2008) 2896–2909.
- [26] M. Shameem, H. Lee, P.P. DeLuca, A short-term (accelerated release) approach to evaluate peptide release from PLGA depot formulations, *AAPS PharmSci* 1 (3) (1999) 1–6.
- [27] Y.M. Ju, B. Yu, L. West, Y. Moussy, F. Moussy, A dexamethasone-loaded PLGA microspheres/collagen scaffold composite for implantable glucose sensors, *J. Biomed. Mater. Res.* 93A (2010) 200–210.
- [28] L. Xiang, W. Bin, J. Huali, J. Wei, T. Jiesheng, G. Feng, L. Ying, Bacterial magnetic particles (BMPs)-PEI as a novel and efficient non-viral gene delivery system, *J. Gene Med.* 9 (2007) 679–690.
- [29] I.S. Kim, S.K. Lee, Y.M. Park, Y.B. Lee, S.C. Shin, K.C. Lee, I.J. Oh, Physicochemical characterization of poly(L-lactic acid) and poly(D, L-lactide-co-glycolide) nanoparticles with polyethyleneimine as gene delivery carrier, *Int. J. Pharm.* 298 (2005) 255–262.
- [30] C.G. Oster, N. Kim, L. Grode, L. Barbu-Tudoran, A.K. Schaper, S.H. Kaufmann, T. Kissel, Cationic microparticles consisting of poly(lactide-co-glycolide) and polyethyleneimine as carriers systems for parental DNA vaccination, *J. Control. Release* 104 (2005) 359–377.
- [31] A.O. Abbas, M.D. Donovan, A.K. Salem, Formulating poly(lactide-co-glycolide) particles for plasmid DNA delivery, *J. Pharm. Sci.* 97 (2007) 2448–2461.
- [32] A. Macchetta, I.G. Turner, C.R. Bowen, Fabrication of HA/TCP scaffolds with a graded and porous structure using a camphene-based freeze-casting method, *Acta Biomater.* 5 (2009) 1319–1327.
- [33] H. Yuan, K. Kurashina, J.D. de Bruin, Y. Li, K. de Groot, X. Zhang, A preliminary study on osteoinduction of two kinds of calcium phosphate ceramics, *Biomaterials* 20 (1999) 1799–1806.
- [34] H.H. Horch, R. Sader, C. Pautke, A. Neff, H. Deppe, A. Kolk, Synthetic, pure-phase beta-tricalcium phosphate ceramic granules (Cerasorb) for bone regeneration in the reconstructive surgery of the jaws, *Int. J. Oral Maxillofac. Surg.* 35 (2006) 708–713.
- [35] M.R. Appleford, S. Oh, J.A. Cole, D.L. Carnes, M. Lee, J.D. Bumgardner, W.O. Haggard, J.L. Ong, Effects of trabecular calcium phosphate scaffolds on stress signaling in osteoblast precursor cells, *Biomaterials* 28 (2007) 2747–2753.
- [36] I.H. Jo, K.H. Shin, Y.M. Soon, Y.H. Koh, J.H. Lee, H.E. Kim, Highly porous hydroxyapatite scaffolds with elongated pores using stretched polymeric sponges as novel template, *Mater. Lett.* 63 (2009) 1702–1704.
- [37] M.R. Appleford, S. Oh, N. Oh, J.L. Ong, In vivo study on hydroxyapatite scaffolds with trabecular architecture for bone repair, *J. Biomed. Mater. Res.* 89A (2009) 1019–1027.
- [38] H. Shen, X. Hu, F. Yang, J. Bei, S. Wang, Combining oxygen plasma treatment with anchorage of cationized gelatin for enhancing cell affinity of poly(lactide-co-glycolide), *Biomaterials* 28 (2007) 4219–4230.
- [39] Y. Wan, X. Qu, J. Lu, C. Zhu, L. Wan, J. Yang, J. Bei, S. Wang, Characterization of surface property of poly(lactide-co-glycolide) after oxygen plasma treatment, *Biomaterials* 25 (2004) 4777–4783.
- [40] J.J. Yoon, J.H. Kim, T.G. Park, Dexamethasone-releasing biodegradable polymer scaffold fabricated by a gas-foaming/salt-leaching method, *Biomaterials* 24 (2003) 2323–2329.
- [41] M.J. Tsung, D.J. Burgess, Preparation and characterization of gelatin surface modified PLGA microspheres, *AAPS Pharm Sci* 3 (2001) E11.
- [42] C. Brochhausen, R. Zehbe, B. Watzler, S. Halstenberg, F. Gabler, H. Schubert, J. Kirkpatrick, Immobilization and controlled release of prostaglandin E2 from poly-L-lactide microspheres, *J. Biomed. Mater. Res.* 91A (2009) 454–462.
- [43] H. Schacke, W.D. Docke, K. Asadullah, Mechanisms involved in the side effects of glucocorticoids, *Pharmacol. Ther.* 96 (2002) 23–43.
- [44] H. Kim, H.W. Kim, H. Suh, Sustained release of ascorbate-2-phosphate and dexamethasone from porous PLGA scaffolds for bone tissue engineering using mesenchymal stem cells, *Biomaterials* 24 (2003) 4671–4679.
- [45] N. Jaiswal, S.E. Haynesworth, A.I. Caplan, S.P. Bruder, Osteogenic differentiation of purified, culture-expanded human mesenchymal stem cells in vitro, *J. Cell. Biochem.* 64 (1997) 295–312.
- [46] H.A. Awad, Y.D. Halvorsen, J.M. Gimble, F. Guilak, Effects of transforming growth factor beta 1 and dexamethasone on the growth and chondrogenic differentiation of adipose-derived stromal cells, *Tissue Eng.* 9 (2003) 1301–1312.
- [47] C.R. Nuttelman, M.C. Tripodi, K.S. Anseth, Dexamethasone-functionalized gels induce osteogenic differentiation of encapsulated hMSCs, *J. Biomed. Mater. Res.* 76A (2005) 1483–1495.
- [48] Q. Wang, J. Wang, Q. Lu, M.S. Detamore, C. Berklund, Injectable PLGA based colloidal gels for zero-order dexamethasone release in cranial defects, *Biomaterials* 31 (2010) 4980–4986.